A new auroral hyperspectral all-sky camera

Fred Sigernes [1,*], Yuriy Ivanov [2], Sergey Chernouss [3], Trond Trondsen [4], Alexey Roldugin [3], Yury Fedorenko [3], Boris Kozelov [3], Andrey Kirillov [3], Vladimir Safargaleev [3] Margit Dyrland [1], Dag Lorentzen [1] and Kjellmar Oksavik [1]

[1] The University Centre in Svalbard (UNIS), N-9171 Longyearbyen, Norway
[2] Main Astronomical Observatory, National Academy of Sciences, Ukraine
[3] Polar Geophysical Institute, Murmansk Region, Apatity, Russia
[4] Keo Scientific Ltd., Calgary, Alberta, Canada
** Corresponding author: fred@unis.no*

Abstract: A prototype auroral hyperspectral all-sky camera has been constructed that uses electro-optical tunable filters to image the night sky as a function wavelength in the visible with no moving mechanical parts. The core optical system includes a new high power all-sky lens with F-number equal to f/1.1. The camera is capable of detecting a few *kR* aurora at an exposure time of only 100 ms.

OCIS codes: (120.4800) Optical Standards and testing; (300.6550) Spectroscopy, visible; (150.1488) Calibration; (350.0350); Astronomical optics; (350.6090) Space optics.

References and links

1. W.L. Wolfe, *Introduction to Imaging Spectrometers*, (SPIE Press, Bellingham, Washington, 1997).
2. F. Sigernes, D.A. Lorentzen, K. Heia, and T. Svenøe, "A multi-purpose spectral imager", Applied Optics **39** (18), 3143 – 3153 (2000).
3. P. J. Miller, "Use of Tunable Liquid Crystal Filters to Link Radiometric and Photometric Standards", Metrologia **28**, 145 – 149 (1991).
4. F. Sigernes, J.M. Holmes, M. Dyrland, D.A. Lorentzen, S. Chernouss, T. Svenøe, J. Moen, and C.S. Deehr, "Absolute calibration of optical devices with a small field of view", Journal of Optical Technology **74**, 669 – 674 (2007).
5. D. Baker and G. Romick, "The Rayleigh: interpretation of the unit in terms of column emission rate or apparent radiance expressed in SI units", Applied Optics **15**, 1966 – 1968 (1976).
6. F. Sigernes, M. Dyrland, N. Peters, D.A. Lorentzen, T. Svenøe, K. Heia, S. Chernouss, C.S. Deehr and M. Kosch, "The absolute sensitivity of digital colour cameras", Optics Express **17** (22), 20211 – 20220 (2009).

1. Short background

During the last decade Liquid Crystal Tunable Filters (LCTFs) have been developed by the company CRi (Cambridge Research & Instrumentation, Inc.). The ability to electronically tune the band pass wavelength of these filters throughout the visible electromagnetic spectrum makes them an ideal candidate for hyperspectral imaging [cf. 1, 2].

A high throughput all-sky lens has been constructed to match the optical design of a LCTF from CRi with an EMCCD (Electron Multiplying Charge Coupled Device) detector from the company Princeton Instruments (PI). This paper describes the optical design and performance of the assembled instrument as candidate for low light hyperspectral imaging of aurora and airglow.

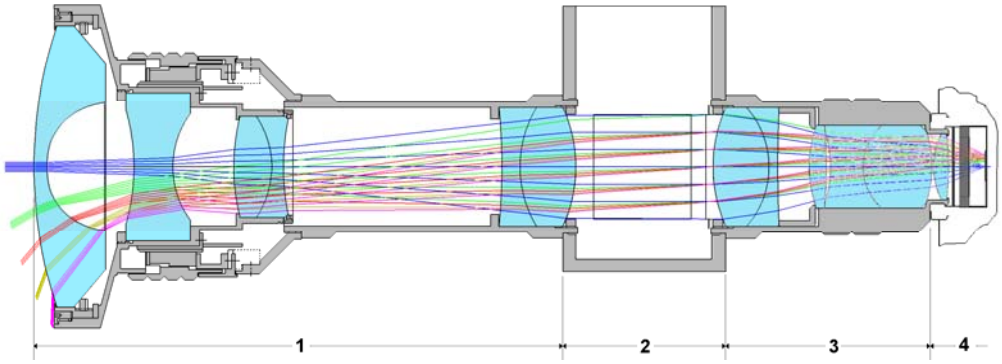

Fig.1. Lens mechanics and optical diagram of the NORUSCA II all-sky lens: (1) focusing mechanism and collimator lenses, (2) filter box - chamber, (3) camera lens, and (4) camera head.

2. Optical layout and design

Fig.1 shows the optical diagram and the lens mechanics of the all-sky lens, named NORUSCA II. The design includes a section or chamber where the light is nearly parallel before it's focused onto the detector. See label (2) in Fig. 1. The circular fish-eye view of the lens is converted by the first part of the lens into a narrow beam of only ±7º. The effective aperture of optical elements that may be inserted into the filter chamber is 35 *mm*. The third part of the lens focuses the light from the filter chamber onto a circular image of 8 *mm* in diameter. The back focal length of the system is 17.5 *mm*, which is compatible with C-mount camera systems.

Note that there is no telecentric lens system in the design. This reduces the number of active optical elements needed to only 12 compared to a standard auroral telecentric all-sky lens system with 19 optical elements. As a consequence, the throughput is increased due to less transmission losses and high effective apertures. The net result is a high throughput all-sky lens with F-number close to one. Table 1 lists the key technical characteristics of the lens.

Table 1. Technical characteristics of the NORUSCA II all-sky lens

NORUSCA II-E fish-eye lens specifications	
Spectral range	430 – 750 *nm*
Paraxial focal length	3.5 *mm*
F-number	f/1.1
Number of lens elements	12
Field of view	180º (circular)
Resolution	80-100 *lp/mm*
Filter diameter	35 *mm*
Angle of incident on filter	< ±7 º
Dimensions	Ø110 × 320 *mm*
Camera lens mount	C-mount

The filter chamber of the lens is matched in size to the LCTF filter. The acceptance angle of 7.5º and the effective aperture of 35 *mm* of the filter are matched to the input light beam divergence cone and its cross section diameter, respectively. The etendue is in other words conserved through the whole system.

Spectral tuning is obtained by using electronically controlled liquid crystal wave plates to a Lyot filter design [cf. 3]. The wave plates behave as optical birefringent elements with an electrically variable retardance. The latter is controllable due the effect that the liquid crystal molecules are orientation sensitive to electric fields applied between the plates. Since the retardance is directly linked to wavelength, the filters are tunable.

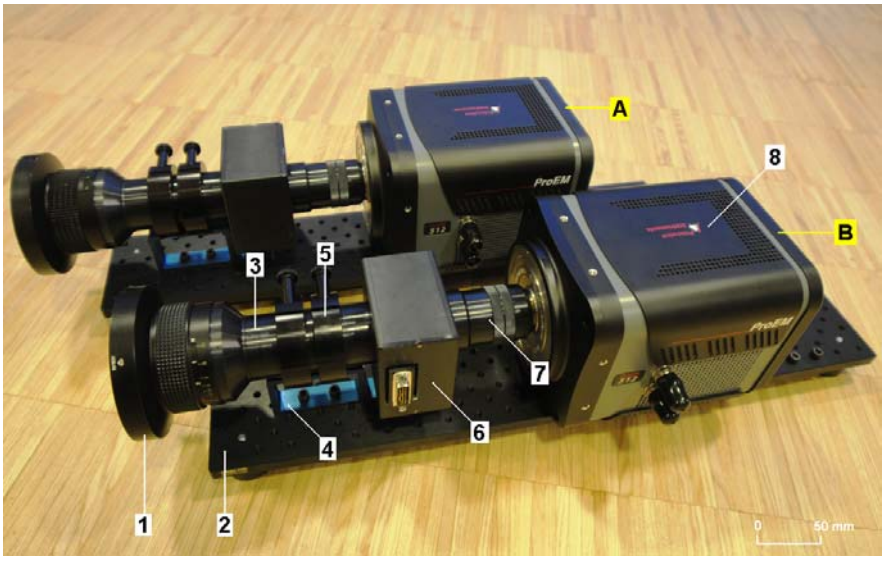

Fig.2. Two NORUSCA II 1st Generation all-sky cameras (A) and (B). (1) Front element of all-sky lens, (2) 24 x 4 inch^2 mount plate, (3) collimator lens tube, (4) lens mount, (5) ring holders, (6) LCTF filter box, (7) camera lens, and (8) EMCCD detector. Instrumental volume is ~ 65 x 18 x 16 cm^3. Total mass is 8.9 kg.

The spectral range of the filter covers the visible part of the electromagnetic spectrum from 400 – 720 *nm*. The bandwidth is 7 *nm*. The filter switches from one wavelength to another in just 50 *ms*. The transmission factors are ~ 10, 40 and 45% at wavelengths 430, 560 and 630 *nm*, respectively.

The low transmission of the filter, especially in the blue part of the spectrum, is compensated by the use of an EMCCD detector from PI named ProEM 512B. The image sensor is back-illuminated with peak quantum efficiency above 90%. The format of the sensor is 512x512 pixels on a square area of 8.2 x 8.2 mm^2, which covers the circular lens image. The camera head is air cooled down to -70ºC to reduce thermo electrical noise. Fig. 2 shows the whole assembled system.

3. System performance

3.1 Spectral characteristics

The experimental setup for intensity calibration is described in detail [4]. A diffuse re-emitting Lambertian screen is located a distance of z = 8 *m* from a standard 45W tungsten lamp (ORIEL SN7-1633). In our case, only the on-optical axis center pixel of the camera is used in order to maker sure that its field of view is filled by the screen. Note that as long as the field of view of the center pixel is filled, then neither the distance of the camera or the angle to the screen matters. The brightness of the screen as seen by the center pixel is given as

$$M_\lambda = B_\lambda \times \rho_\lambda \times \left(\frac{z_0}{z}\right)^2, \quad [mW\,m^{-2}\,nm^{-1}] \tag{1}$$

where the subscript λ refers the wavelength. B_λ is the known radiance (certificate) of the tungsten lamp, initially obtained at a distance z_0 = 0.5 *m*. ρ_λ is the hemispherical spectral reflectance factor of the Lambertian surface (Labsphere Inc. SRT-99-180). The reflectance factors are nearly constant throughout the visible spectrum *(ρ_λ =0.98)*.

A mercury vapor tube supplied by Edmund Optics Ltd. /SN K60-908) is used for wavelength calibration of the camera. The mercury lamp is used as source to the screen. Note that the source for our calibration is the screen, not the lamps by them self.

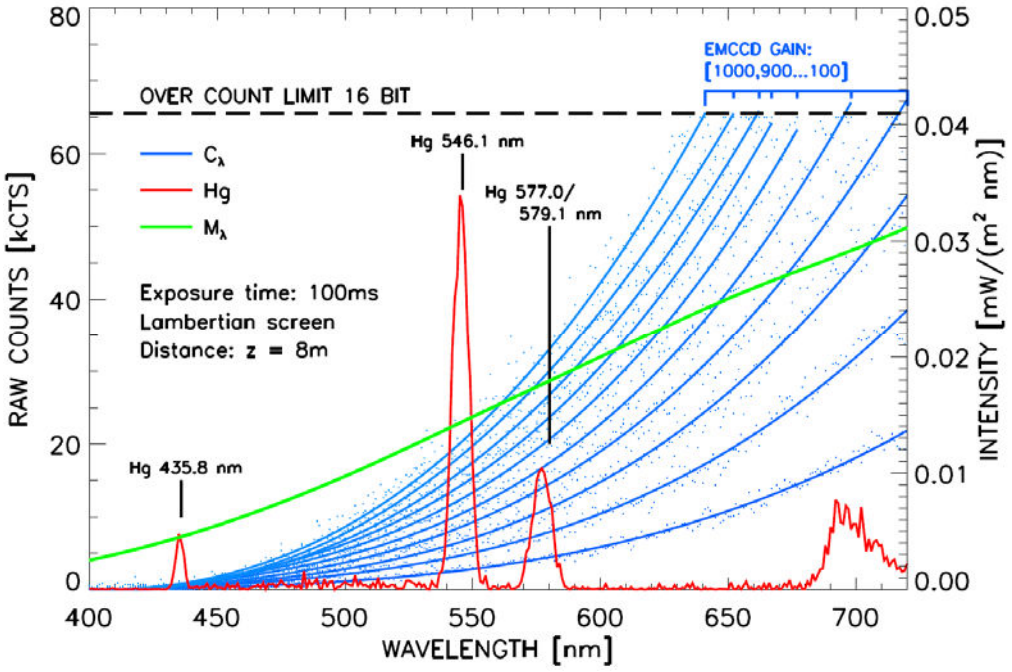

Fig.3. The NORUSCA II camera on-optical axis center pixel spectral characteristics. The spectra, C_λ, (blue solid curves) are 3rd order polynomial fits to the raw data (blue dots) as a function of detector gain. The source is a Lambertian surface (Labsphere SRT-99-180) illuminated by *45W* tungsten lamp (ORIEL SN7-1633) at a distance of *z=8 m*. The green spectrum, M_λ, is the intensity of the screen in absolute units of $mW\ m^{-2}\ nm^{-1}$. The red spectrum is from a mercury vapor tube supplied by Edmund Optics Ltd (SN K60908). Exposure time is 100 *ms*.

Fig. 3 shows the results of the calibration. The wavelength calibration shows that the peak emissions of mercury, Hg 425.8 *nm*, Hg 546.1 *nm* and the 477.0/579.1 *nm* doublet are all identified within the measured Full Widths at Half Maximum (FWHM) of 3.71 *nm*, 6.86 *nm* and 8.85 *nm*, respectively. The FWHM increases with wavelength, and the nominal FWHM = 7 *nm* at center wavelength 550 *nm*, as reported by CRi, is close to our results. The close match indicates that the lens elements are aligned according to theory.

Next is the sensitivity calibration. Fig. 3 shows the spectral raw counts C_λ of the center pixel as a function of EMCCD gain, ranging from 100 up to 1000 in steps of 100. The exposure time was kept fixed at 100 *ms*. A 3rd order polynomial fit is applied to each spectrum. The overall counts are increasing exponentially with wavelength. This is mainly due to the 45*W* tungsten lamp, which peaks in the near infrared part of the spectrum at $\lambda =$ 900 *nm*. Also as expected, the noise levels increase with gain. The standard deviations of the raw counts from the polynomial fits are ±376 and ±1456 for gain equal to 100 and 1000, respectively.

With focus on aurora, screen brightness is converted to Rayleigh (*R*) [5], the calibration factor is given as

$$K_\lambda = 20.1106 \times \lambda \times \left(\frac{M_\lambda}{C_\lambda} \right), \quad [R\,Å^{-1} CTS^{-1}] \tag{2}$$

where the wavelength λ is in units of Ångstrøm (*Å*) and M_λ in units of $mW\ m^{-2}\ nm^{-1}$. Eq. (2) is plotted for 3 auroral wavelengths in Fig. 4 panel (A). The blue emission line at 4861 *Å* is from proton impact excitation of hydrogen (H_β), while the green 5577 *Å* and the red 6300 *Å* emissions are due to electron impact excitation of atomic oxygen (*O*).

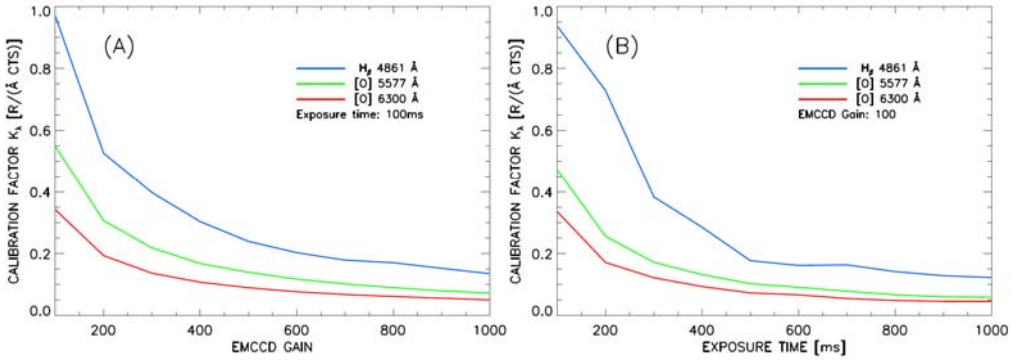

Fig.4. Panel (A): Center pixel calibration factors of the NORUSCA II camera as a function of EMCCD gain at auroral wavelengths H_β 4861 *Å* (blue), [*O*] 5577 *Å* (green) and [*O*] 6300 *Å* (red). Exposure time is fixed at 100 *ms*. Panel (B): Calibration factors as a function of exposure time. Gain is set to 100.

The calibration factors are relatively high for low gain values, converging down to a more stable level above gain = 500. As an example, a raw data count of 1000 *CTS* at gain = 1000 results in an auroral red intensity of 0.05 $R\ Å^{-1}\ CTS^{-1}$ x 1000 *CTS* x 97 *Å* = 4.8 *kR* at wavelength 6300 *Å*. The corresponding green intensity at 5577 *Å* is 5.4 *kR*, and the blue intensity at 4861 *Å* is 7.3 *kR*. In the latter calculations, it is assumed that the instrumental profiles are triangular with FWHM equal to 56, 77 and 97 *Å* for the 4861, 5577 and 6300 *Å* emission lines, respectively. These intensities are classified as weak aurora, and the camera detects it at an exposure time of only 100 *ms*.

The above procedure has been repeated as a function of exposure time. See panel (B) of Fig. 4. The gain was in this case fixed to 100 with exposure times ranging from 100 to 1000 *ms*. The results are surprisingly equal to using the gain as free variable. The main difference is that the noise level is reduced, which opens for even longer exposure times. Our screen is simply too bright.

3.2 Focus test

In order to test focus of the camera, a pinhole of 1 *mm* in diameter is back illuminated by a LED (Light Emitting Diode). A neutral density filter (SCHOTT ND96) in front of the pinhole is used to attenuate the intensity by a factor of 0.96. The pinhole is located at a distance of 1 *m* from the center of the front surface of the all-sky lens on an arm that can be rotated an angle θ with respect to the optical axis. In this configuration, the pinhole acts as artificial star with an angle θ to the optical axis.

First the pinhole was positioned at the optical axis with $\theta = 0^{\circ}$, in the center of the image. Exposures were taken at wavelengths 4861, 5577 and 6300 *Å* as a function of object distance defined by the lens. Fig. 5 show intensity slices along the horizontal direction (x-axis) of the pinhole at object distances set to infinity (∞), 2.0 *m*, 1.0 *m* and 0.7 *m*. For all 3 wavelengths the sliced profiles peak when we reach focus. In our case, this is at object distances between ∞ and 2 *m*. The shape of the profiles depends highly on focus point. In focus, the profiles are narrow and triangular. The FWHM of the triangles is 2 pixels. As we loose focus, the profiles become less intense, more smeared out and shifted to the left.

Secondly, …

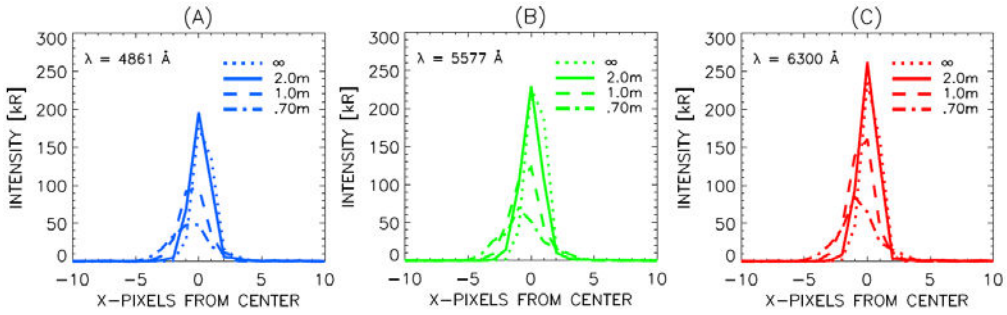

Fig.5. Focus test of the NORUSCA II camera. The source is a LED in front of a 1 *mm* in diameter pinhole that is attenuated by a neutral density filter, located 1 *m* from the camera (on optical axis). Lens object distance settings are set to ∞, 2 *m*, 1 *m* and 0.7 *m*. Panels (A), (B) and (C) show the sliced intensities of the pinhole at center wavelengths 4861, 5577 and 6300 *Å*, respectively. Exposure time is fixed at 1000 *ms* and gain is 100.

4. Concluding remarks

The principal results obtained by this study can be summarized as follows.

(1) A new camera system for imaging….

(2) The sensitivity …

Acknowledgement

This work was financially supported by The Research Council of Norway through the project named: Norwegian and Russian Upper Atmosphere Co-operation On Svalbard part 2 # 196173 / S30 (NORUSCA2).